IEICE TRANS. ELECTRON., VOL.E100–C, NO.5 MAY 2017

PAPER Special Section on Fundamentals and Applications of Advanced Semiconductor Devices

An Improved EEHEMT RF Noise Model for 0.25 μm InGaP pHEMT Transistor Using Verilog-A Language

An-Sam PENG[†a)], ***Member and*** **Lin-Kun WU**[†], ***Nonmember***

SUMMARY In this paper, an accurate experimental noise model to improve the EEHEMT nonlinear model using the Verilog-A language in Agilent ADS is presented for the first time. The present EEHEMT model adopts channel noise to model the noise behavior of pseudomorphic high electron mobility transistor (pHEMT). To enhance the accuracy of the EEHEMT noise model, we add two extra noise sources: gate shot noise and induced gate noise current. Here we demonstrate the power spectral density of the channel noise S_{id} and gate noise S_{ig} versus gate-source voltage for 0.25 μm pHEMT devices. Additionally, the related noise source parameters, i.e., P, R, and C are presented. Finally, we compare four noise parameters between the simulation and model, and the agreement between the measurement and simulation results shows that this proposed approach is dependable and accurate.

key words: *pHEMT, noise parameters, modeling, EEHEMT*

1. Motivation and Background

The pseudomorphic high electron mobility transistor (pHEMT) features high carrier mobility because of its two-dimensional electron gas, making it highly qualified for applications with higher frequencies up to millimeter-wave applications, such as switches and power amplifiers. The superior gain and noise performance of pHEMT devices also make them suitable for low-noise amplifier (LNA) applications [1]. To exploit the utmost efficiency and to save chip area, monolithic microwave integrated circuit (MMIC) designers need an accurate and easy convergence model. Therefore, Agilent EEsof developed a large-signal EEHEMT model to describe the behaviors of the pHEMT [2]. The advantage of this mature and industrial standard model is that it provides higher modeling accuracy in I–V and transconductance (g_m) curves [3]. Several studies have adopted the EEHEMT model and have good fitting results [4]–[6]. Another commonly used Angelov model is especially suitable for switch modeling because of its high orders differentiable property. With the scaled-down pHEMT gate lengths, short channel effects are becoming more obvious. Because channel noise in the EEHEMT model considers only the long channel case [7], we need to take into account the short-channel effects on the noise model. This accurate model will help MMIC designers achieve the best value in the trade-off between low noise and high gain. In this paper, we propose an improved noise model based on the EEHEMT model and implemented it using the Verilog-A language [8]–[10]. Although we demonstrate this method only for 0.25 μm InGaP pHEMT, this method can still be applied to other gate lengths.

Manuscript received August 26, 2016.
Manuscript revised December 27, 2016.

[†]The authors are with the Department of Electrical Engineering, National Chiao-Tung University, Hsinchu, 300, Taiwan.
a) E-mail: 15208206945@163.com

DOI: 10.1587/transele.E100.C.424

2. Improved EEHEMT Noise Model

Figure 1 shows the equivalent circuit of improved EEHEMT model with proposed added noise sources, we turn off the noise generated by original channel noise and the thermal noise produced by the resistors Ris, Rid, and Rdb, but keep the inherent resistors Rg, Rs, and Rd. Besides; we add three noise sources to the intrinsic circuit of the EEHEMT model: channel noise current $\overline{i_d}$, gate shot noise current $\overline{i_{gs}}$ [11], induced gate noise current $\overline{i_g}$, as well as their cross-correlation noise $\overline{i_g i_d^*}$. The gate shot noise is caused by random passage of individual charge carriers across a potential barrier. Channel noise is a kind of thermal noise generated by random motion of free carriers between drain and source. This random potential fluctuation in the channel will also cause the induced gate noise through the capacitive coupling between channel and gate. Therefore, induced noise is correlated with channel noise. Here, we used Verilog-A to implement these two correlated noise sources. The original

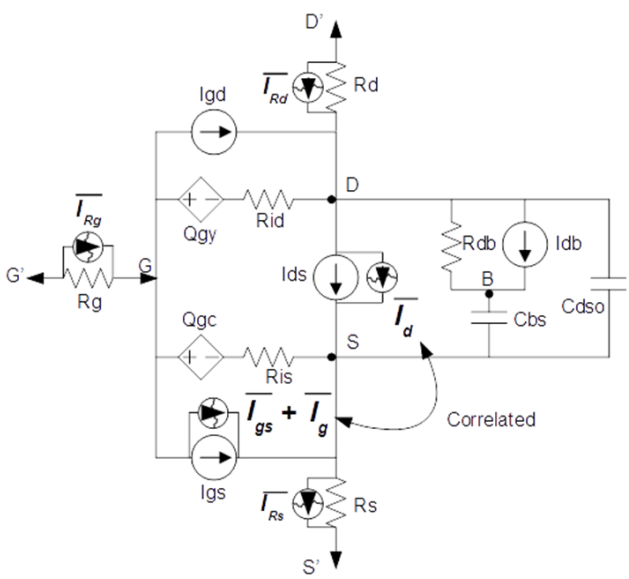

Fig. 1 Equivalent circuits for improved EEHEMT noise model with proposed added noise sources.

channel noise of the EEHEMT model is calculated by the following spectral density:

$$S_{id} = \frac{\overline{i_d^2}}{\Delta f} = \frac{8kTg_m}{3} \tag{1}$$

where $\overline{i_d}$ is the channel noise current, k is Boltzmann's constant, T is the ambient temperature in Kelvin, Δf is the noise bandwidth, and g_m is the DC transconductance. According to this equation, the shape of the channel noise in the EEHEMT model is similar to the g_m. Obviously, this simple formula is often not enough to precisely predict noise characteristics of pHEMTs. Therefore, a measurement approach based on S-parameter and RF noise measurement has been presented [12]. This method needs to establish the equivalent small-signal model first, and then it can calculate two-port admittance Y_{intr} of the intrinsic part in the RF transistor model [13]. Finally, refer to the equations from 16 to 18 of paper [12] directly to obtain the S_{id}, S_{ig} and S_{igd*}.

$$\frac{\overline{i_g^2}}{\Delta f} = 4kTR_nY_{21,intr}^2 \tag{2}$$

$$\frac{\overline{i_d^2}}{\Delta f} = 4kTR_n\{\, Y_{opt}^2 - Y_{11,intr}^2 + 2R[(Y_{11,intr} - Y_{cor})Y_{11,intr}^*]\,\} \tag{3}$$

$$\frac{\overline{i_d i_g^*}}{\Delta f} = 4kT(Y_{11,intr}^2 - Y_{cor})R_nY_{21,intr}^* \tag{4}$$

this paper also add gate leakage noise current on the terminals of the gate and source. The shot noise can be estimated from the equation

$$i_{gs}(t) = \sqrt{2qI_G\Delta f} \tag{5}$$

where I_G is the DC leakage current of gate. Here, we can directly use the Agilent Advanced Design System (ADS) to simplify extraction steps. Because the thermal noises of resistances and gate shot noise have been determined from EEHMET model parameters, we change $\overline{i_d}$, $\overline{i_g}$ and $\overline{i_g i_d^*}$ to fit measured noise parameters, including minimum noise figure (NFmin), unnormalized noise resistance (Rn) and optimum source impedance which corresponds to NFmin (Γopt). The advantage of this approach is that the original EEHEMT model simulation behavior of DC and small-signal does not change, only the noise parameters of the simulation change. Next we adopt a physical-based presentation of noise characteristics. That is, the two most-common correlated noise sources in the PRC model [14], which can be directly linked to the physical processes and the related power spectral densities of the noise source, are listed as follows:

$$S_{id} = \frac{\overline{i_d^2}}{\Delta f} = 4kTg_mP \tag{6}$$

$$S_{ig} = \frac{\overline{i_g^2}}{\Delta f} = 4kT\frac{(\omega C_{gs})^2}{g_m}R \tag{7}$$

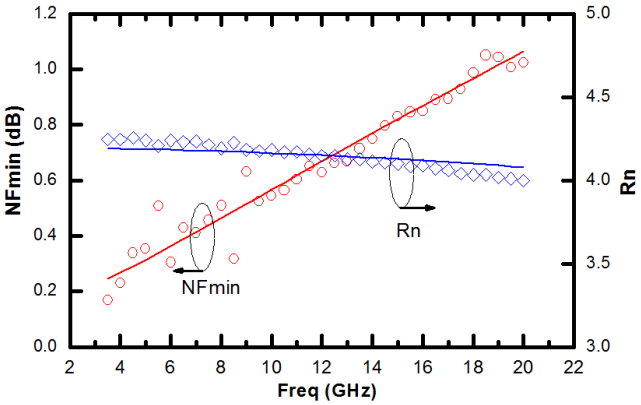

Fig. 2 Frequency dependence of minimum noise figure (NFmin) and Rn between modelled and measured data at Vds = 3 V and Vgs = 0.5 V.

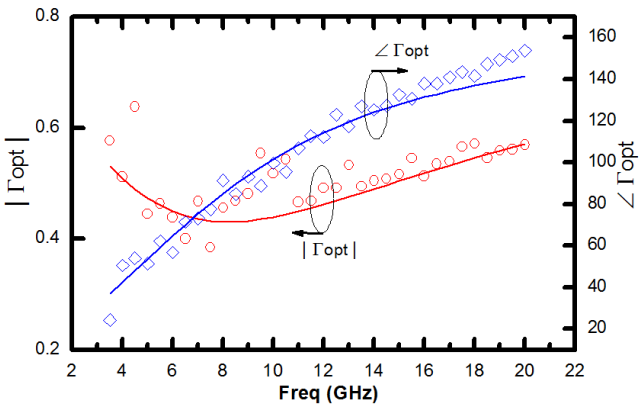

Fig. 3 Frequency dependence of |Γopt| and ∠Γopt between modelled and measured data at Vds = 3 V and Vgs = 0.5 V.

$$S_{igd*} = \frac{\overline{i_d i_g^*}}{\Delta f} = jC\sqrt{\overline{i_d^2}\cdot\overline{i_g^2}} \tag{8}$$

where S_{ig} is the gate-induced noise, and P and R represent the channel noise resulting from the charge fluctuation and gate noise induced from the channel noise, respectively. In addition, jC is the correlation coefficient between these two noise sources. The imaginary j means that the 90^o phase shift resulting from the induced gate noise is coupled through the gate-channel capacitance. This measurement is carried out by the Focus noise parameter measurement system [15], which uses an electro-mechanical tuner to vary the input reflection presented to the device, and then calculates four noise parameters using its proprietary algorithm. Noise and the S-parameter were measured in the frequency range from 1 to 26 GHz using a PNA-X network analyzer [16], calibrated by the Short-Open-Load-Thru method. Because the frequency of less than 5 GHz, the NFmin of pHEMT device is too low to obtain the correct value. Besides, the difference between hot and cold powers of our noise source is less obvious when frequencies higher than 20 GHz. We extract noise sources in the range of 5 GHz to 20 GHz. The method we used is to change S_{id}, S_{ig0} and C to get the best fit of the four measured noise parameters in the frequency range of 5 GHz to 20 GHz. Figure 2 and 3 show the results

of frequency dependence of modelled and measured noise parameters at Vds = 3 V and Vgs = 0.5 V. Here the fitting results are: S_{id} = 1.45e−021, S_{ig0} = 2.7082e−25 and C = 0.7875. We can improve the accuracy of EEHEMT noise model if we have accurate noise measurement data. Device under test was fabricated in enhancement/depletion (E/D) mode PHEMT process, which obtains cutoff frequency (ft) of 45 GHz and maximum oscillation frequency (fmax) of 70 GHz, with 0.25 μm gate length, 50 μm gate width and six gate finger numbers. This is because the parasitic resistance of drain and source is inversely proportional to gate width, but too wide gate width also increases the gate resistance (distribution effect). Using the parallel of finger numbers is a good way to reduce parasitic resistance, but too many finger numbers will also result in phase mismatch and higher metal parasitic resistance problems. Because the LNA design mainly uses positive voltage to reduce cost, the noise model of this paper is established only for the case of enhancement mode (normally-OFF device). Figure 4 shows the typical DC characteristics of this device under the bias condition of Vds = 2.8 V (Vdso). Here, Vdso is an important parameter of EEHEMT model that used to represent vds-dependence of model equations [2]. The Vdso-Vds terms in some equations, such as Ids (drain-source current) and g_m (transconductance) can be simplified, that is, there is no longer Vds-dependence. Figure 5 shows the S_{id} of the extracted results of the improved model. The S_{id} of the improved model increases as the gate-source voltage increases. The reason for the discrepancy of S_{id} is that S_{id} of EEHEMT model is only proportional to g_m, whereas S_{id} of this improved paper is proportional to g_m multiplied by P. Therefore, this improved model can obtain more accurate fitting results. Moreover, this improved model also includes induced gate noise and gate shot noise to enhance the noise model accuracy.

3. Results and Discussion of Experiments

Figure 6 shows that S_{id} increases as the gate-source voltage increases. Here, we sweep the gate-source voltage (Vgs) from 0.35 to 0.65 V at drain-source voltages (Vds) of 3 V and 4 V. In this paper, S_{ig0} (A^2/Hz) is defined as the value of S_{ig} at 1 GHz and replace the S_{ig} mainly because it simplify the expression of source noise Verilog-A. Both S_{id} and S_{ig0} increases rapidly with the increasing Vgs. The only difference between S_{id} and S_{ig} versus Vgs is that Vds has an obvious influence on S_{ig0}. Figure 7 shows the model parameters P, R, and C versus Vgs. We can observe that P first

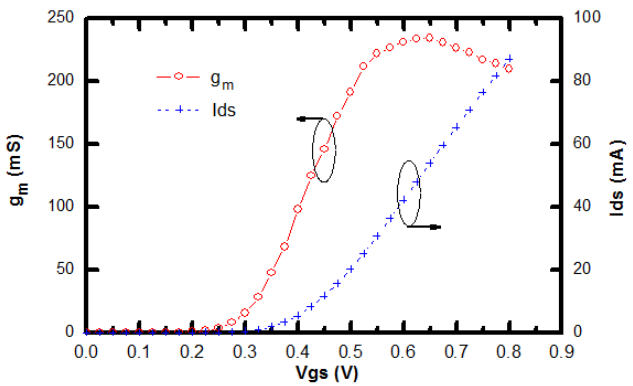

Fig. 4 Drain current and transconductance versus gate-source voltage.

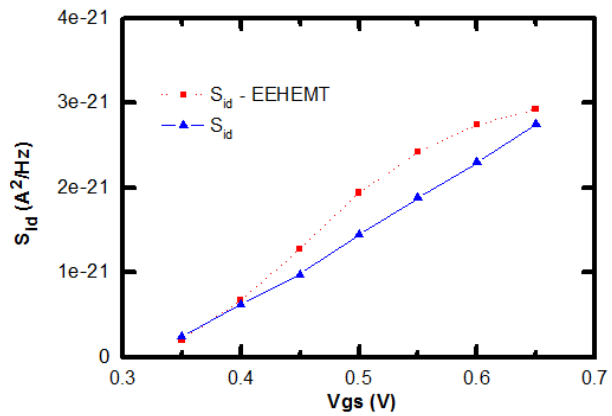

Fig. 5 Channel noise versus gate-source voltage between extracted results (triangles) and EEHEMT model (squares).

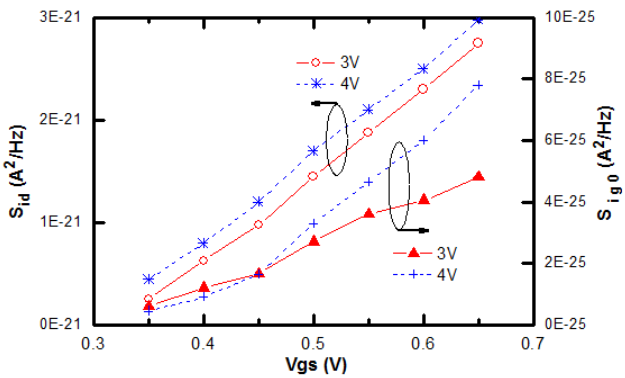

Fig. 6 Extracted channel noise and induced gate noise versus gate-source voltage.

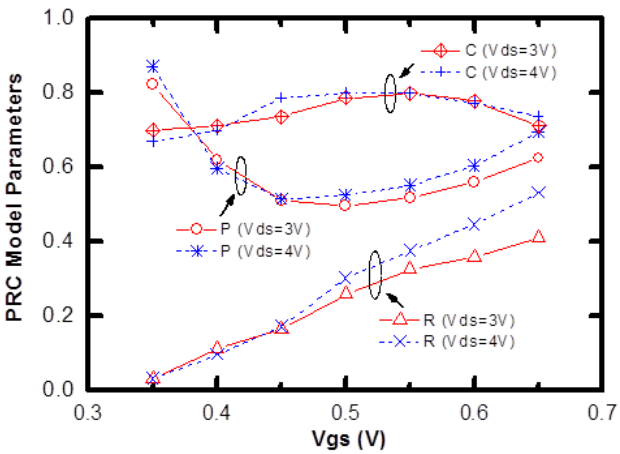

Fig. 7 Model parameters P, R, and C versus Vgs.

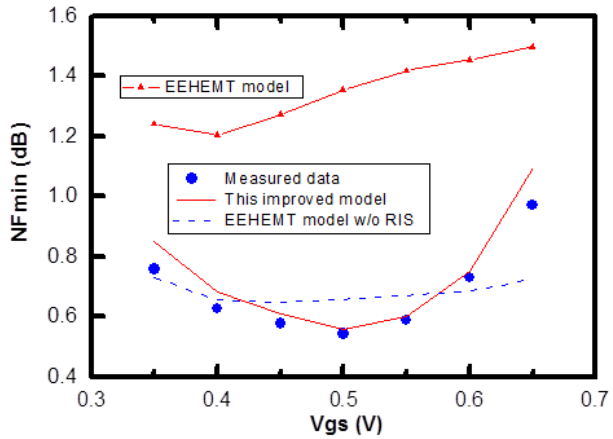

Fig. 8 Measured data (dots) and simulation results with different model of NFmin versus Vgs.

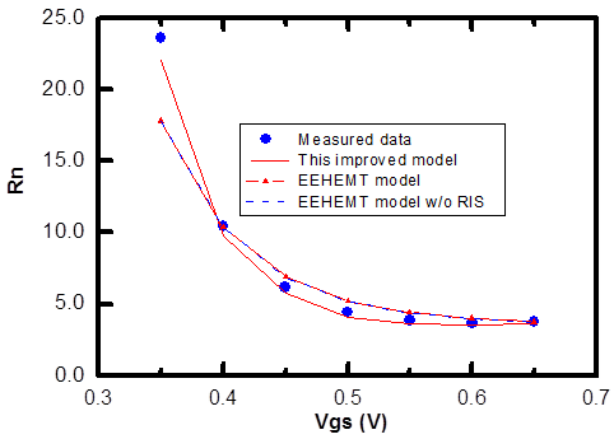

Fig. 9 Measured data (dots) and simulation results with different model of Rn versus Vgs.

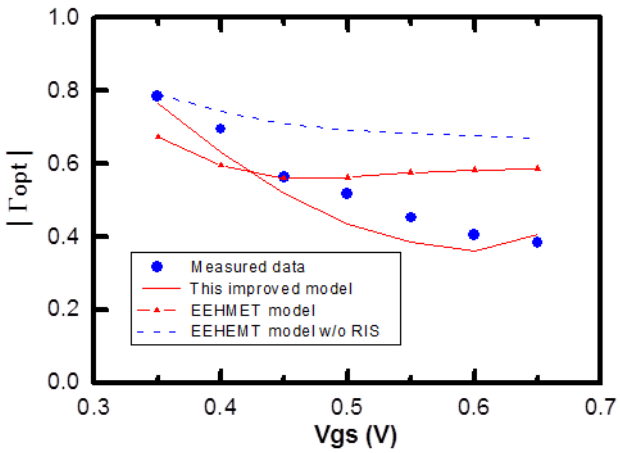

Fig. 10 Measured data (dots) and simulation results with different model of |Γopt| versus Vgs.

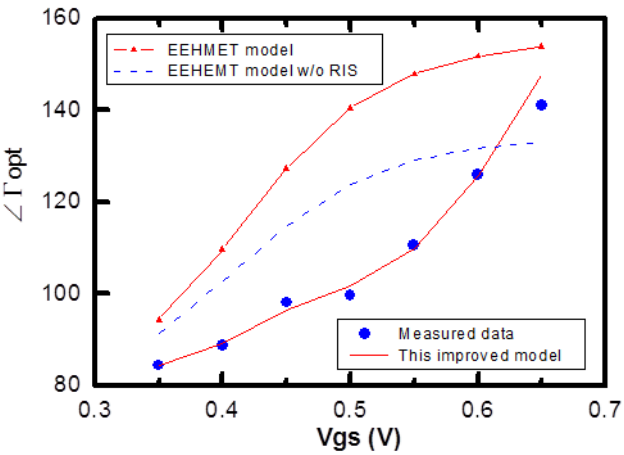

Fig. 11 Measured data (dots) and simulation results with different model of ∠Γopt versus Vgs.

decreases and then increases with increasing Vgs. This typical U-shape is caused by P being inversely proportional to the drain current at low Vgs (ohmic region) and directly proportional to current at high Vgs (saturation region) [17]. In addition, R increases with increasing Vgs, which is similar to a previous study [17]. Here, C is an inverted U-shape as a function of Vgs, and description of an inverted U-shape requires a complicated model equation. Finally, we verify the RF noise model accuracy between our improved model and the EEHEMT model through noise parameter prediction. Figure 8 shows that the EEHEMT model obviously overestimates the NFmin, which is mainly caused by the thermal noise of the intrinsic source resistance (Ris). The Agilent EEHEMT model adopts the intrinsic source and drain resistance (Ris and Rid) to model the charging delay between the channel and the depletion region. The respective default values of Ris and Rid are 6 and 0.1 Ω. Therefore, the high value of Ris inevitably raises the NFmin. Moreover, even though we neglect the Ris, the improved model has better-fitting results than the EEHEMT model. Here, we can see that the NFmin obviously follows the typical smiling curve form. The lowest NFmin occurred at approximately Vgs = 0.5 V. Unlike NFmin, Ris has only a small influence on Rn, as shown in Fig. 9. The EEHEMT and improved model both exhibit high accuracy. NFmin and Rn are considered to be figures of merit for the noise figure; this is mainly because Rn represents the sensitivity of the noise figure and varies with source impedance change. That means a low Rn can tolerate high process variation. Figure 9 shows the device has a low Rn when Vgs > 0.5 V. Finally, we check the accuracy of the source impedance for the minimum noise figure. Although this is not the figure of merit for device performance, it is still important for an RF designer to match the source impedance to 50 Ω. Figures 10 and 11 show that the improved model can enhance the accuracy of the EEHEMT model, especially on the angle of Γopt.

4. Implementation Technique Using Verilog-A

Because ADS can load the Verilog-A modules to execute user-defined equations [18], we implemented this improved model with the Verilog-A language in the ADS simulation

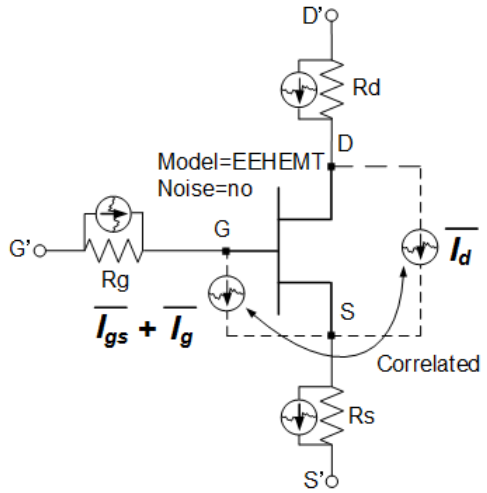

Fig. 12 The improved EEHEMT noise model implemented by Verilog-A

system. The greatest advantage of this method is that we can improve the noise accuracy of the EEHEMT without varying the DC and RF characteristics and the customer's habit of using the ADS. Here, we can use the white_noise() function of Verilog-A to generate uncorrelated noise. It can transform the frequency-independent PSD into the time domain as follows:

$$white\_noise(S_i) = F^{-1}(\sqrt{S_i}) = \sqrt{S_i(t)} \tag{9}$$

In addition, we also use the ddt(x) time-derivative function to generate a frequency dependence that is directly proportional.

$$F\left(\frac{d}{dt}a(t)\right) = j \cdot 2\pi f \cdot A(f) \tag{10}$$

Next, we can define the noise current:

$$i_d(t) = white\_noise((1 - C^2) \cdot S_{id}) + C \cdot white\_noise(S_{id}) \tag{11}$$

$$i_g(t) = ddt\left(\frac{1}{2\pi \cdot 10^9}\sqrt{\frac{S_{ig0}}{S_{id}}} \cdot white\_noise(S_{id})\right) \tag{12}$$

Consequently, we can derive the following results:

$$F(i_d(t)) \cdot F(i_d(t))^* = S_{id} \tag{13}$$

$$F(i_g(t)) \cdot F(i_g(t))^* = f^2 \cdot 10^{-18} \cdot S_{ig0} \tag{14}$$

$$\frac{F(i_g(t)) \cdot F(i_d(t))^*}{|F(i_g(t))| \cdot |F(i_d(t))|} = jC \tag{15}$$

Figure 12 shows the diagrammatic sketch for the implementation of the improved EEHEMT noise model. It comprises the following steps:

Step 1: Move the Rd, Rs, and Rg resistances of the EEHEMT model from the inside to outside. This means that we duplicate these resistances outside the EEHEMT model and set the internal resistance values to zero. Our main aim is to turn off the internal noise and replace it with the Verilog-A module. At the same time, we keep the thermal noise generated by the resistances.

Step 2: Add a parallel channel noise current to flow from the drain to the source terminal. In terms of the EEHEMT model, because the Rd and Rs resistances have been moved outside, the additional noise current is the same as that directly added to the channel.

Step 3: Mount the above induced gate and gate leakage noise current on the terminals of the gate and source. The shot noise can be estimated from

$$i_{gs}(t) = \sqrt{2qI_G\Delta f} \tag{16}$$

where I_G is the DC leakage current of gate. We can define two short-circuit terminals to detect the gate current with an ammeter. Accordingly, the modeling engineer can give the value of S_{id}, S_{ig}, and C according to the measurement and fitting results. Finally, we need to link the Verilog-A module to the ADS user interface. The associated Verilog-A source code is attached in the appendix.

5. Conclusion

This paper has demonstrated how to implement an improved model with the Verilog-A language in ADS. We also analyzed how the noise characteristics vary with different gate-source voltages. The measurement and simulation results achieved close agreement for the four noise parameters. Thus, this improved the EEHEMT RF noise model that is reliable and realizable.

References

[1] T. Padmaja, R.S. N'Gongo, P. Ratna, P.S. Vasu, J.S. Babu, and V.S.R. Kirty, "A 18 - 40GHz Monolithic GaAs pHEMT low noise amplifier," Proc. IEEE Conf. Recent Adv. Microw. Theory and Appl., Jaipur India, pp.309–311, Nov. 2008.

[2] Agilent EEHEMT1 Model Equations http://edadocs.software.keysight.com/display/iccap2012/Agilent+EEHEMT1+Model+Equations

[3] L.-S. Liu, J.-G. Ma, and G.-I. Ng, "Electrothermal Large-Signal Model of III-V FETs Including Frequency Dispersion and Charge Conservation," IEEE Trans. Microw. Theroy Tech., vol.57, no.12, Dec. 2009.

[4] Y.H. Chang and J.J. Chang, "Analysis of an EEHEMT Model for InP pHEMTs," Proc. IEEE Conf. Electron Devices and Solid-State Circuits, pp.237–240, Dec. 2007.

[5] J. Dhar, S.K. Garg, R.K. Arora, and S.S. Rana, "Nonlinear Design of a C band Power Amplifier using EEHEMT Nonlinear Model," Proc. 19th Mixed Design of Integr. Circuits and Syst. Conf., pp.360–363, May 2012.

[6] S. Eskanadri and F.T. Hamedani, "Extracting the Parameters of an EEHEMT Nonlinear Model for InP HEMT Operating at G-band Frequency," Proc. IEEE Conf. Electron Devices and Solid-State Circuits, pp.237–240, Dec. 2007.

[7] EE_FET3_Model (EEsof Scalable Nonlinear GaAsFet Model) http://edocs.soco.agilent.com/display/ads201101/EE+FET3+Model+(EEsof+Scalable+Nonlinear+GaAsFet+Model)

[8] Verilog-AMS Language Reference Manual http://www.verilog.org/verilog-ams/htmlpages/public-docs/lrm/2.2/VAMS-LRM-2-2.pdf

[9] C. McAndrew, G. Coram, W. Grabinski, A. Blaum, and O. Pilloud,

"Correlated noise modeling and simulation," Proc. 8th Workshop. on Compact Modeling. Anaheim, California, USA. p.4045, May 2005.
[10] "A Verilog-A Implementation for Correlated Noise in HBTs" http://ectm.ewi.tudelft.nl/publications_pdf/110111_SAFE2010.pdf
[11] R. Reuter, S. van Waasen, and F.J. Tegude, "A New Noise Model of HFET with Special Emphasis on Gate-Leakage," IEEE Electron Device Lett., vol.16, no.2, pp.74–76, Feb. 1995.
[12] C.-H. Chen, M.J. Deen, Y. Cheng, and M. Matloubian, "Extraction of the Induced Gate Noise, Channel Noise, and Their Correlation in Submicron MOSFETs from RF Noise Measurements," IEEE Trans. Electron Device, vol.48, no.12, pp.2884–2892, Dec. 2001.
[13] G. Dambrine, A. Cappy, F. Heliodore, and E. Playez, "A New Method for Determining the FET Small-Signal Equivalent Circuit," IEEE Trans. Microwave Theory Tech., vol.36, no.7, pp.1151–1159, July 1988.
[14] R.A. Pucel, H.A. Haus, and H. Statz, "Signal and noise properties of GaAs microwave FET," Advances in Electron. & Electron Physics, vol.38, pp.195–265, New York: Academic Press, 1975.
[15] Noise Parameter System http://www.focus-microwaves.com/integration
[16] N5242A PNA-X Microwave Network Analyzer, 26.5 GHz http://www.keysight.com/zh-CN/pd-867173-pn-N5242A/pna-x-microwave-network-analyzer?cc=CN&lc=eng
[17] B.-U.H. Klepser, C. Bergamaschi, M. Schefer, C.G. Diskus, W. Patrick, and W. Bachtold, "Analytical Bias Dependent Noise Model for InP HEMT's," IEEE Trans. Electron Devices, vol.42, no.11, pp.1882–1889, Nov. 1995.
[18] Using Verilog-A and Verilog-AMS in Advanced Design System http://edocs.soco.agilent.com/display/ads201101/Using+Verilog-A+and+Verilog-AMS+in+Advanced+Design+System

Appendix: Verilog-A Source Code

```
'include "disciplines.vams"
'include "constants.vams"
'define QQ 1.602e-19
module VCNC_2P_equation(p1, p2, p3, p4, ref5, ref6, p7);
inout p1, p2, p3, p4, ref5, ref6, p7;
//Note: p1 = G, p2= D, ref5=S (Terminals in Figure 12)
//Note: p3 = G', p7= D', ref6=S'
//Note: short between p3 and p4 to obtain I_G
electrical p1, p2, p3, p4, ref5, ref6, p7, imt1, imt2;
...
analog begin
vds = V(p7,ref6);
vgs = V(p3,ref6);
...
//Note: Implementation of equation 9 - 11
sid = a1 + b1 * exp(vgs); //Note: A^2/Hz (white value)
sig0 = 1e-26 * exp(a2+b2/vgs/vgs);
ci= a3 + ( b3 / ( 1 + exp(-( vgs - c3 + d3/2) / e3))) * ( 1-
1/(1+exp(-( vgs - c3 - d3/2 ) / f3 )));
//Note: fitting parameters at Vds = 4 V
//Note: a1=-6.82778E-21; b1=5.132E-21; a2=5.6417321;
//Note: b2=-0.5469797;a3=0.66818424;b3=0.1375;c3=0.53466368;
//Note: d3=0.23075;e3=0.016127;f3=0.0377381;
...
sigr = sqrt(sig0/(freq0*freq0*1e18)/sid) / (2*3.1415926);
...
V(imt1) <+ white_noise((1-ci*ci)*sid);
V(imt2) <+ white_noise(sid);
...
//Note: Implementation of equation 8 and shot noise
I(p1,ref5) <+ ddt(sigr*V(imt2))+white_noise(2*1.6e-19
*abs(I(p3,p4)));
//Note: Implementation of equation 7
I(p2,ref5) <+ V(imt1)+ci*V(imt2);
...
end
endmodule
```

An-Sam Peng was born in Hsinchu, Taiwan, in 1976. He received a B.S. in electronics engineering from Feng Chia University, Taichung, Taiwan, in 1999, and an M.S. degree in electrical engineering from the National Chung Hsing University, Taichung, Taiwan, in 2001. He is currently pursuing the Ph.D. degree in communication engineering at the National Chiao Tung University, Hsinchu. His current research interests focus on RF De-embedding technique and device modeling.

Lin-Kun Wu was born in Hsinchu, Taiwan, in 1958. He received the M.S. and Ph.D. degrees in electrical and computer engineering from the University of Kansas, Lawrence, in 1982 and 1985, respectively. From November 1985 to December 1987, he was a Postdoctoral Research Associate with the Center for Research Inc., University of Kansas, where he was involved with microwave remote sensing and computational electromagnetics. Since 1988, he has been with the Department of Communication Engineering, National Chiao Tung University, Hsinchu, where he is currently a Professor. His current research interests include computational electromagnetics, biological effects and medical applications of electromagnetic energy, and electromagnetic compatibility.